Online Anomaly Detection in DC/DC Converters by Statistical Feature Estimation Using GPR and GA

Yueming Jiang, Yang Yu, *Senior Member, IEEE*, and Xiyuan Peng

***Abstract*—DC/DC converters play an important role in electrical systems. The anomalous state of a dc/dc converter has a major impact on the operation of the back-end components and the entire electrical system. To effectively recognize an anomalous state, particularly for dc/dc converters with unknown circuit structures, an online anomaly detection method that involves statistical feature estimation using Gaussian process regression (GPR) and a genetic algorithm (GA) is proposed. In the proposed method, the normal output range is built upon the dc/dc normal output signal using GPR, and seven statistical features are considered as the detection indexes. In the detection process, the output signal of the dc/dc converter is acquired, and the corresponding extreme values of statistical features are calculated by using GA, which can effectively reduce the operation time and the calculation consumption. The working state of the dc/dc converter is distinguished according to these features. Simulation and hardware experimental results validate the practicability and effectiveness of the proposed method.**

***Index Terms*—DC/DC converter, Gaussian process regression (GPR), genetic algorithm (GA), online anomaly detection, statistical feature estimation.**

I. Introduction

DC/DC converters have been widely applied in many electrical devices, including test instruments, large-scale computers, and biomedical instruments. Such converters fundamentally ensure electrical devices operating in their normal states. The reliability of a dc/dc converter, which has a strong influence on the working state of the back-end components and the entire electrical system [1], [2], depends on the performance of its components. With the increasing operation time, the performance of the components including the electrolytic capacitor, power devices, and inductance, etc., will degrade under many types of stresses such as the voltage, temperature, humidity, and radiation stresses [3]. For example, the capacitance and equivalent series resistance (ESR) of an electrolytic capacitor will gradually decrease and increase [4], [5]. These situations can cause the dc/dc converter working anomalously, or even affect the entire electrical system. If the anomalous states in a dc/dc converter are not effectively identified and prevented, the likelihood that the anomaly develops into the sudden circuit failure will increase, which can ultimately cause enormous economic loss. Therefore, it is necessary and urgent to effectively detect anomalies in dc/dc converters.

In recent years, many studies focused on detecting and diagnosing the faults of dc/dc converters. These fault detection and diagnosis methods can be divided into two categories: model-based techniques and data-driven techniques.

Model-based methods establish the relationships between the outputs and the degradation parameters, and they are mainly applied to the dc/dc converters with the known circuit structure. For example, in [6]–[8], the mathematical relationship between the instantaneous capacitor voltage and the degradation parameters was analyzed according to the circuit structures of the Flyback converter, buck converter, and PFC converter. Meanwhile, the additional circuits including the online monitoring system were required. In [9] and [10], Ahmad *et al.* proposed techniques to monitor the ESR and the low-frequency impedance of an electrolytic capacitor in a PV-based dc system. The method in [9] needed a high sampling frequency. To decrease the sampling frequency, a low-frequency current ripple was injected into the capacitor [10]. However, the injection signal would have some effect on the normal outputs of the back circuits. Janne *et al.* [11] proposed an output voltage transient step response analysis method to detect capacitor wear-out at the output stage of a step-down dc/dc converter. The estimation accuracy of the degradation capacitance was dependent on the measurement accuracy and the noise floor level, so the robustness was not very high. Hiroshi *et al.* [12] presented a new method for a digitally controlled switching mode power supply to estimate the ESR from the output voltages with a step load change. Amaral and Cardoso [13] proposed a simple online fault detection technique that was able to prevent structural failures in aluminum electrolytic capacitors used in the output filter of step-down dc/dc converters. In [14], the article presented a fast yet robust method for fault diagnosis in nonisolated dc/dc converters. Summarizing the aforementioned literatures, one critical condition of applying the model-based technique to estimate anomalous states is knowing the dc/dc converter structure very well. Moreover, other conditions include the additional circuits or an excitation source, which may increase the test cost and have some effect on the normal output of dc/dc converter.

In practical applications, the circuit structures of dc/dc converters are usually unknown. Therefore, data-driven methods

Manuscript received July 11, 2019; revised October 28, 2019 and February 2, 2020; accepted March 7, 2020. Date of publication March 16, 2020; date of current version June 23, 2020. This work was supported by the National Natural Science Foundation of China under Grant 61571161. Recommended for publication by Associate Editor Dr. John Lam. *(Corresponding author: Yang Yu.)*

The authors are with the School of Electronics and Information Engineering, Harbin Institute of Technology, Harbin 150080, China (e-mail: yueming07050106@163.com; yuyanghit@hit.edu.cn; pxy@hit.edu.cn).

Color versions of one or more of the figures in this article are available online at http://ieeexplore.ieee.org.

Digital Object Identifier 10.1109/TPEL.2020.2981500

are applied to detect and diagnose the anomalous states. The relationship between the parameters to be estimated and the available signals is established through training data, which are obtained from the output of the dc/dc converter. In [15] and [16], Thanh *et al.* presented a novel condition monitoring scheme for estimating the ESR and capacitance of a dc-link electrolytic capacitor in three-phase ac/dc pulsewidth modulation converters and PWM inverter-fed induction machine drives, respectively. Then, a recursive least-squares algorithm was implemented to obtain the degradation parameters. An artificial neural network (ANN) was trained in [17] and [18] to form a mapping between the inputs and outputs of a power electronic circuit and to estimate the capacitance. In [19], a method was suggested for online estimating and tracking both the capacitance and ESR using the ratio between the capacitors voltage ripple and their current ripple. Additional data-preprocessing modules were also needed. Khalila *et al.* [20] presented an identification model based on support vector regression, and the relation between a known capacitor power and its corresponding capacitance was established. The above studies established the relationships between the degradation parameters and outputs of a dc/dc converter using data-driven methods, such as ANN and SVM. These methods required both normal samples and fault samples or abnormal samples as the training data. Thus, the detection accuracy of the data-driven methods depends on the accuracy of these training data, especially abnormal samples. Moreover, the fault samples or abnormal samples are usually insufficient under the actual operation, so these samples are mainly obtained from simulation experiments. However, differences must exist between the fault samples obtained from the simulation experiments and those extracted from the actual applications. These situations impair the accuracy of the data-driven methods.

The detailed information of the existing techniques are shown in Table I. The current techniques in these literatures mainly belong to the model-based [6]–[14] and date-driven methods [15]–[20]. A few methods [21]–[23] do not exactly belong to these two methods. Analyzing the comparison results in Table I, limitations and demerits of these methods still exist and are concluded as follows.

1) Some research works mainly concentrate on building the models to estimate or identify the component parameters, such as the capacitance and ESR of the electrolytic capacitor. The estimation results of these models may be influenced by the accuracy of these models and the interference from the environment. Moreover, for detecting the anomalies caused by the weak parameters variation in dc/dc converter, likewise the stresses, noises, and loads, the effectiveness of the above methods may be impractical.

2) In some studies, additional circuits will increase the test cost, for an example, test excitation and test point are inserted into the circuits.

3) The methods based on the model are only suitable to the dc/dc converter with the known circuit structure. For the data-driven methods, the high fault detection accuracy depends on sufficient abnormal or fault samples.

Based on the aforementioned analysis, it is necessary to propose an anomaly detection method that has the capability to detect the anomalous states caused by the weak parameters degradation of the components as well as the environmental stresses. Low-test cost and great practicability are also two important advantages, which means the method can be implemented economically and fulfill the actual industrial requirement.

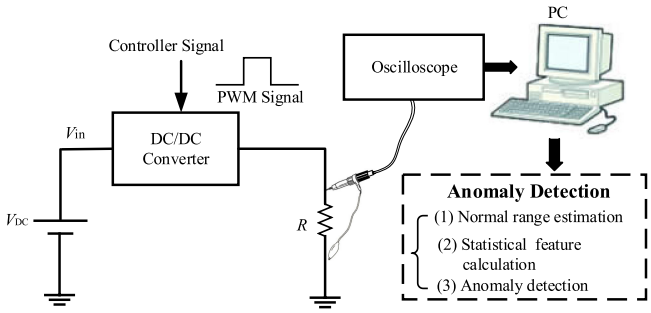

Fig. 1. Principle of the online anomaly detection method.

In this article, an anomaly detection method by statistical feature estimation using GPR and GA is proposed. The main principle of the proposed method are as follows. At first, the method adopts Gaussian process regression (GPR) to estimate the normal output range, and building the GPR model requires only normal samples obtained from actual circuits as the training data. Then, seven statistical features of the output are calculated by a genetic algorithm (GA), and the extreme values of features are saved as detection indexes. Anomaly detection is implemented by comparing the seven statistical features of the actual output with those saved detection indexes. When one of the features deviates from these indexes, it provides an indication that the working state of the dc/dc converter has become abnormal.

Compared with the existing methods mentioned in Table I, the proposed method has three merits. First one is detecting more anomalous types and fault components, especially for the weak parametric faults of all components. Second one is no need the test point, test exaction, and additional test circuits, the test cost is low. Third one is no need the structure of the dc/dc converter. The proposed method has great practicability in the actual applications.

This article is organized as follows. Section II presents the principle of the proposed online anomaly detection method. The experiments and analysis are shown in Section III to further validate the merits of the proposed method, different comparison experiments will be conducted. Meanwhile, the hardware experiments are used to demonstrate the practicability of this method. Finally, Section IV concludes the article.

II. Method of Online Anomaly Detection in the DC/DC Converter

The online anomaly detection process is shown in Fig. 1. For a dc/dc converter, the input and output signals are dc signals, and the PWM signal is used as the controller signal of the MOSFET. The oscilloscope acquires the output signals of dc/dc converter. The output signal at the initial operation stage is regarded as

TABLE I
INFORMATION OF THE EXISTING TECHNIQUES

Ref.	Fault description			Test cost			Circuit structure
	Fault type	Fault component	Fault causes in the experiments	Test point	Test Excitation	Additional test structure	
[6]	Parametric fault	Electrolytic capacitor	*	*	*	1. Pulse capture circuit 2. Ripple voltage isolation amplifier 3. Input and output voltage sampling circuits	Known
[7]	Parametric fault	Electrolytic capacitor	*	*	*	1. Trigger circuit 2. Isolation and amplification circuit	Known
[8]	Parametric fault	Electrolytic capacitor	*	*	*	1. Trigger circuit 2. Current and Voltage isolated amplifiers	Known
[9]	Parametric fault	Electrolytic capacitor	*	*	*	1. DSP 2. Ripple extraction circuit	Known
[10]	Parametric fault	Electrolytic capacitor	1.2 times of the initial low-frequency impedance	Adding two points	Low-frequency current ripple	1. MPPT module 2. Voltage and current controllers 3. PWM modulator	Known
[11]	Parametric fault	Electrolytic capacitor	-30% capacitance -30% L +300% ESR	*	*	1. STM32F407 microcontroller 2. Spartan 6 FPGA	Known
[12]	Parametric fault	Electrolytic capacitor	-20% or -40% capacitance +25% or +40% ESR Four times of the initial value ESR	*	*	1. MPU 2. Anti-Aliasing Filter	Known
[13]	Parametric fault	Electrolytic capacitor	Twice of the ESR	*	*	*	Known
[14]	Open and Short Fault	Switch	OCF with a small duty ratio D SCF with D close to 80%	Adding one point	*	1. FPGA 2. Two paralleled FD subsystems	Known
[15]	Parametric fault	Electrolytic capacitor	*	*	Ac current component	Temperature measurement circuit	Unknown
[16]	Parametric fault	Electrolytic capacitor	*	*	Current injection	*	*
[17]	Parametric fault	Electrolytic capacitor Diode	ESR from 0.1 to 0.5 Diode on-state voltage from 0.4 to 0.8	*	*	*	Unknown
[18]	Parametric fault	Electrolytic capacitor	*	*	*	*	Unknown
[19]	Parametric fault	Electrolytic capacitor	*	*	Ac voltage with a lower frequency	A/D and D/A converters	Unknown
[20]	Sudden fault	Electrolytic capacitor	-39.39% capacitance +300% ESR	*	*	1. Data preprocessing for the output voltage and current 2. Current sensor	Unknown
[21]	Open and short fault Paramedic fault	Transistor Electrolytic capacitor	*	Adding one test point	*	1. Rogowski coil sensor 2. Gate driver circuit	Known
[22]	Open faults	Diodes Transistor	*	Adding one test point	*	Drives	Unknown
[23]	Open and Short faults	Transistor	*	Adding one test point	*	1. Transformer 2. An auxiliary winding in the magnetic core 3. Inductor	*

"*" means that the relative information are not mentioned in the corresponding references.

the training samples. Then, the normal output range will be estimated and the seven statistical features will be calculated. The entire one-time calculation is implemented by MATLAB software on a PC and the seven features will be saved as the detection indexes. During the online anomaly detection process, only output signal acquisition and simple index comparison are implemented. The detailed principle of the anomaly detection method are as follows.

A. Normal Output Range Estimated Based on the GPR Model

In this article, GPR is used to estimate the normal output range. It will reduce the reliance on the fault samples, because building a GPR model requires only normal samples obtained from actual circuits as the training data. The estimated normal output range is taken as the key criterion to detect an anomaly. In general, GPR is defined as a collection of a finite number of random variables $\{f(t_i)|t_i \in t\}$ indexed by a set t. The stochastic process is specified by giving the probability distribution for every finite subset of variables $f(t_i)$ in a consistent manner [24].

For a dc/dc converter, t is the input space with dimension time indexes, which is the number of inputs of the training data. $f(t_i)$ is a one-dimensional dataset that represents the output signal x_i, i.e., the outputs of the training data, which are the normal output samples, and the inputs of the testing data are the index values of the actual output to be detected. The Gaussian process $f(t)$ can be fully described by the mean function $m(t)$ and covariance function $k(t, t')$, which are defined as follows:

$$m(t) = E(f(t)) \tag{1}$$

$$k(t, t') = E[(f(t) - m(t)) \cdot (f(t') - m(t'))]. \tag{2}$$

GPR can be described as $f(t) \sim GP[m(t), k(t, t')]$. To ensure a high anomaly detection ability, it is necessary that the

covariance function can describe all waveform trends of the normal output of the dc/dc converter. In this study, according to the waveform trends of the output of the dc/dc converter, the combination covariance function is used to increase the anomaly detection ability. The first condition is that the output signal must be periodic, the period equals to that of the PWM signal controlling the MOSFET transistor. Therefore, a periodic covariance function should be used to form the combination covariance function because of the periodic output signal which can be defined as

$$k_{\mathrm{PER}}(t,t') = \sigma_1^2 \exp\left[-\frac{2}{l_1^2}\sin^2(\pi(t-t')/p)\right]. \tag{3}$$

The dc output signal also continually fluctuates because of the ripple. The squared exponential covariance function, as a common covariance function, is used to form the combination covariance function

$$k_{\mathrm{SE}}(t,t') = \sigma_2^2 \exp\left[\frac{(t-t')^2}{2l_2^2}\right] \tag{4}$$

where σ_1^2 and σ_2^2 are the vertical scaling factors that adjust the change of the covariance function. l_1 and l_2 are the horizontal scaling factors that have a relative weighting effect on the distance between the input points t and t'. The parameter p adjusts the estimation period.

Therefore, a periodic covariance function is combined with a squared exponential covariance function to obtain a combination covariance function, which can achieve the normal output range with superior estimation performance in a dc/dc converter. The combination covariance function k_{C} is defined as follows:

$$\begin{aligned} k_{\mathrm{C}}(t,t') &= k_{\mathrm{PER}}(t,t') + k_{\mathrm{SE}}(t,t') \\ &= \sigma_1^2 \exp\left[-\frac{2}{l_1^2}\sin^2(\pi(t-t')/p)\right] \\ &\quad + \sigma_2^2 \exp\left[\frac{(t-t')^2}{2l_2^2}\right]. \end{aligned} \tag{5}$$

In summary, the modeling process based on GPR for dc/dc converter is as follows.

Step 1: Choose the initial normal output as the training data and the online real-time output as the testing data.

Step 2: Construct the combination covariance function, including a period covariance function and a squared exponential function.

Step 3: Set the initial values of hyperparameters, and establish *a priori* model of GPR.

Step 4: Use the training data to train *a priori* model of GPR, and optimize the hyperparameters.

Step 5: Obtain the optimal hyperparameters and establish *a posterior* model of GPR.

Step 6: Predict the mean values and the variance values of the online real-time output.

B. Statistical Feature Calculation for a DC/DC Converter

The actual output signal of a dc/dc converter is inevitably mixed with noise and interference because of the complex working conditions, which adversely affects the anomaly detection accuracy. To increase the detection accuracy and robustness of the model, statistical features of the output are adopted as detection indexes to identify the anomalous state in this article. This is because when the parameters of the components degrade, it influence the entire tendency of the output. Thus, anomaly detection is realized by comparing seven statistical features of the actual output with those of the estimated normal output range.

Seven statistical features in a dc/dc converter are chosen as detection indexes to analyze the online output. The seven features are the range, mean, standard deviation, skewness, kurtosis, entropy, and centroid of the output signal x, which are designated as r, m, v, s, k, e, and c, respectively.

The range r denotes the change between the maximum and minimum values of the output signal x, namely, the amplitude of the output-ripple voltage, as expressed in (6). $x_{\max}$ is the maximum value of the output signal and $x_{\min}$ is the minimum value

$$r = x_{\max} - x_{\min}. \tag{6}$$

Equations (7) and (8) express the mean and standard deviation of the output signal, respectively. The mean value is the ideal output voltage of a dc/dc converter. The length of the output signal x is n, and $x_i (i = 1, 2, \ldots, n)$ denotes every data point of x

$$m = E(x) = \frac{1}{n}\sum_{i=1}^{n} x_i \tag{7}$$

$$v = \sqrt{E(x-m)^2} = \sqrt{\frac{1}{n-1}\left(\sum_{i=1}^{n} x_i^2 - n\cdot[E(x)]^2\right)}. \tag{8}$$

The skewness, a measure of the asymmetry of the output signal relative to the mean value, is defined as follows:

$$s = E\left[\left(\frac{x-m}{v}\right)^3\right]. \tag{9}$$

The kurtosis is a measure of the heaviness of the tails in the distribution of the output signal x and can be used to establish an effective statistical test for identifying signal changes. Equation (10) expresses the kurtosis in the zero-mean case [25]

$$k = E\{x^4\} - 3[E\{x^2\}]^2. \tag{10}$$

However, it is very challenging to calculate the kurtosis of the output signal of an analog circuit based on (10). Equation (11) gives the unbiased estimation or approximation equation [26]

$$k = \frac{E\{x^4\}}{[E\{x^2\}]^2} = n\cdot\frac{\sum_{i=1}^{n} x_i^4}{(\sum_{i=1}^{n} x_i^2)^2}. \tag{11}$$

The entropy, a fundamental concept in information theory, is also very challenging to calculate from the output signal of an analog circuit. Equation (12) shows the approximation equation of the entropy e [27]

$$e \approx k_1(E\{G^1(x)\})^2 + k_2(E\{G^2(x)\} - \sqrt{1/2})^2 \tag{12}$$

TABLE II
OUTPUT CHANGING RATES BETWEEN THE NORMAL AND ANOMALOUS STATES

	Anomaly state 1	Anomaly state 2	Anomaly state 3	Anomaly state 4	Anomaly state 5
Original signal	0.21%	0.32%	0.01%	0.97%	0.01%
Range	9.75%	18.90%	1.82%	14.02%	1.21%
Mean	0.10%	0.08%	0.03%	0.97%	0.02%
Standard deviation	11.27%	17.85%	0.20%	13.17%	0.16%
Skewness	1.28%	1.45%	2.43%	7.36%	1.47%
Kurtosis	0.46%	0.41%	0.63%	0.10%	0.22%
Entropy	0.03%	0.02%	0.01%	0.40%	0.01%
Centroid	170.49%	53.40%	98.85%	98.00%	106.55%

where $k_1 = 36/(8\sqrt{3}-9)$, $k_2 = 24/(16\sqrt{3}-27)$, $G^1(x) = x\exp(-x^2/2)$, and $G^2(x) = \exp(-x^2/2)$.

The centroid is located in the closed region, which is formed by the waveform of the output signal and abscissa axis. For a zero-mean discrete-valued signal, the centroid can be obtained by

$$c = \frac{\sum_{i=1}^{n} n \times x_i}{\sum_{i=1}^{n} x_i}. \tag{13}$$

When detecting an anomaly in a dc/dc converter, statistical feature calculation can enhance the difference between the normal state and anomalous state and increase the robustness of the detection method. To further demonstrate the advantages of this estimation method, a specific example is presented. For a buck converter, the anomalous states will be caused by the parameter degradation of the electrolytic capacitor and the inductor, etc. C_{normal}, L_{normal}, and $\text{ESR}_{\text{normal}}$ represent the normal capacitance value, inductor value, and ESR of the electrolytic capacitor, respectively. The anomalous states include -10% C_{normal}, -15% C_{normal}, $+20\%$ $\text{ESR}_{\text{normal}}$, -25% L_{normal}, and $+10\%$ $\text{ESR}_{\text{normal}}$, denoted by anomalies 1, 2, 3, 4, and 5, respectively. Two hundred output samples are obtained for each state, with a sampling interval of 1 μs. The output difference between the original signals and the seven statistical features of six states including the normal and all five anomalous states are compared. The difference is defined as (14). V_{normal} means the original output or the statistical features of the normal states. V_{anomaly} means these outputs of the anomalous states. D_{rate} means the anomalous output changing rate compared with the normal outputs

$$D_{\text{rate}} = \left| \frac{V_{\text{normal}} - V_{\text{anomaly}}}{V_{\text{normal}}} \right| \times 100\%. \tag{14}$$

According to (14), Table II shows the results.

In Table II, the relative change rates of five anomalous states are very small when comparing the original outputs between the normal and anomalous states. Then, using the statistical features, most relative change rates are larger than those when using the original outputs, especially the relative change rates of range, standard deviation, skewness, and centroid are great large. In conclusion, the statistical features of the output can be used to characterize the output deviation more clearly than the original outputs.

C. Extreme Values Calculation for Statistic Features of the Normal Range Based on GA

The normal output range can be obtained by GPR, the maximum and minimum values of seven features are needed to acquire. For calculating the extreme values, it is necessary to calculate seven features for each normal output and then to compare these features. However, the normal output range includes numerous normal outputs. Thus, the calculation will be very large and complicated, which will increase the modeling time and the calculation consumption of the proposed method. Meanwhile, the extreme values are used as the detection indexes, which directly determine the anomaly detection accuracy. Hence, the article calculates these extreme values using the GA. Because GA, as an optimum algorithm, not only can reduce the operation time, but also can obtain more accurate extreme values than the randomly sampling output signals mentioned in [28]. The process of GA search is described as follows.

First, set the encoded mode of the output data of every sampling as binary. Each normal output is the gene of the individual, the number of normal outputs is set as N, and the number of sampling points is m. Therefore, the encoded digit n identifies the least positive integer that makes $2^n > N$ reasonable. Every $n \times m$ matrix of binary code represents each normal output. Second, set the fitness function. In each generation, the fitness of every individual in the population is evaluated, which is the value of the fitness function in the optimization problem. Individuals with higher fitness are stochastically selected from the current population. The equation of each statistical feature is the objective function. The fitness function is the exponential form of the objective function with the base of the natural number. Third, design the genetic operators. The type of selected operator is proportionate selection, i.e., roulette-wheel selection. The modes of the crossover operator and mutation operator are single-point crossover and simple mutation, respectively. Finally, the selection process for the extreme values of the seven statistical features is based on the GA as follows.

Step 1: Perform binary encoding and parameter initialization. The parameters include the population, generation, crossover probability, and mutation probability.

Step 2: Calculate the fitness values of the individuals. Each individual expresses each normal output in the estimated normal output range. The genes are selected, crossed, and mutated to produce the new generation.

Step 3: Terminate the algorithm when the maximum number of generations has been produced. The results are the maximum and minimum values of each statistical feature.

Step 4: Compare the seven statistical features of the actual output with the extreme values in the estimated normal output range, and detect any anomaly in the dc/dc converter.

D. Procedure of Online Anomaly Detection

The detailed procedure of the proposed online anomaly detection method is described in Fig. 2.

Step 1: Collect the actual normal outputs of the dc/dc converter used as the training data of GPR.

Step 2: Estimate the reasonable normal output range based on GPR, which is the key criterion to detect the anomaly outputs.

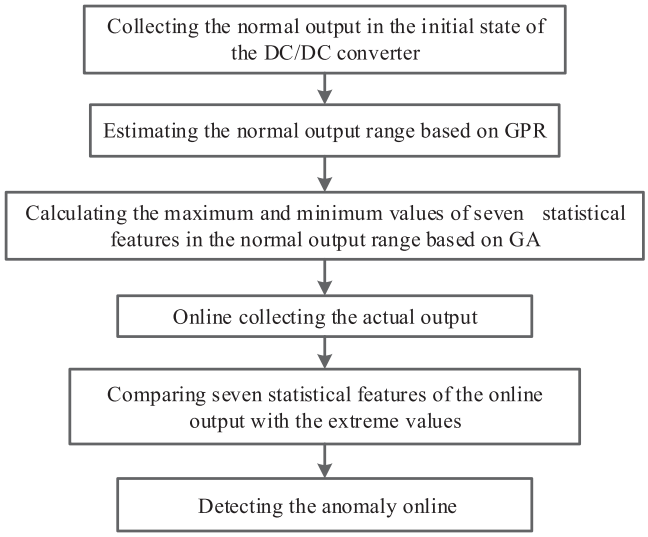

Fig. 2. General diagram of online anomaly detection.

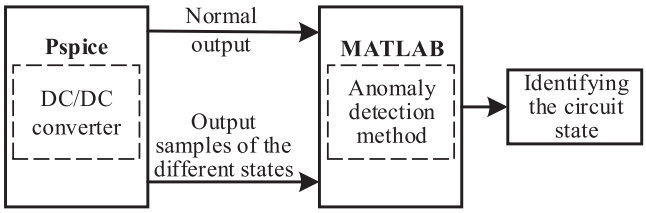

Fig. 3. Simulation experiment process of online anomaly detection.

Step 3: Calculate seven statistical features to describe the output of the dc/dc converter.

Step 4: Utilize the GA to calculate the maximum and minimum values of these features in the estimated normal output range.

Step 5: Compare the seven features of the actual output with the extreme values. The anomaly will be detected online when any one of the seven features of the actual output deviates from the extreme values.

III. Experiments and Analysis

The proposed online anomaly detection method can be applied to a dc/dc converter irrespective of whether the circuit structure is known. To demonstrate the advantages and the validity, the simulation and hardware experiments are conducted.

A. Simulation Experiment Based on PSpice Simulation

When detecting the anomaly, the only needed information is the output samples, both the circuit structure and component parameters of the dc/dc converter are not required. To verify the proposed method by simulation experiment, the component parameters of the chosen experiment circuit structure are aware here for injecting the anomalous states. The simulation experiment process of online anomaly detection is shown in Fig. 3. Buck converter is chosen as the experimental circuit, which is

TABLE III
Parameters of Buck Converter

Parameter	Variable	Value
Input voltage	Vin	+3 V
MOSFET transistor	M	IRF150
Internal resistance of MOSFET transistor	Ron	0.01Ω
Period of PWM signal	PER	40 μs
Pulse width of PWM signal	PW	24 μs
Capacitance of electrolytic capacitor	C	4.7μF
Inductance of inductor	L	110μH
Internal resistance of inductor	RL	0.1 Ω
Internal resistance of diode	Rd	0.01 Ω
ESR of electrolytic capacitor	ESR	0.1 Ω
Output load resistor	R	50 Ω

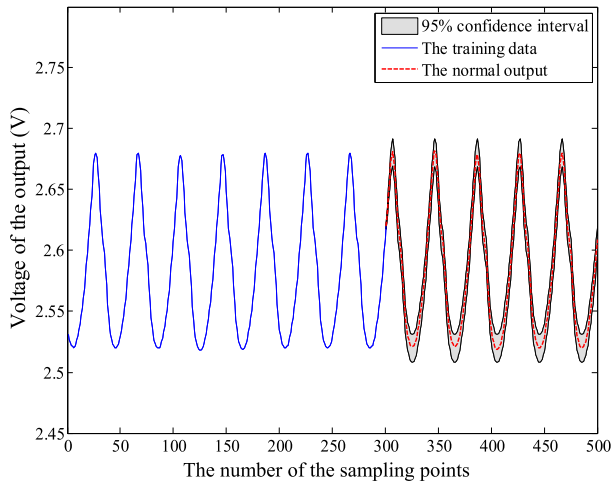

Fig. 4. Estimated normal output range based on the GPR model.

composed by capacitor, resistors, and MOSFET transistor, etc. The tolerance of all components is set to 5%. The amplitude of the input voltage is +3 V. Simulations are conducted using PSpice 16.7. The specifications and parameters of the converter components are given in Table III. The buck converter discussed here is just an example for showing the working procedure of the proposed method. In fact, the proposed method can be extended to various PWM dc/dc converters topologies irrespective of the circuit structure.

The dc/dc converter at the initial operation stage is considered in the normal state. The normal samples are collected as the training data to build the model based on GPR, and the sampling interval is set to 1 μs. According to output of the dc/dc converter, the suitable covariance function and hyperparameter values are selected to make GPR model detect the weak anomalous states and normal states effectively. The estimated normal output range obtained by the GPR model is shown in Fig. 4 using MATLAB.

In Fig. 4, the normal sampling points from 0 to 300 represent the training data, i.e., the normal outputs. For the GPR model, the sampling points from 301 to 500 are used as the testing data. The gray band represents the estimated normal output range, while the red dashed line represents the online normal output. Because the output samples in the normal output obey a Gaussian

distribution, and the mean and square deviations are estimated by GPR, the range of the normal output in this article is set to twice the square deviation, i.e., approximately 95%. This setting demonstrates that the output range of the GPR model has a high identification ability for the normal samples.

To further demonstrate the advantages of the proposed anomaly detection method, four comparison experiments are conducted.

1) Online Anomaly Detection Under The Ideal Condition: Based on a theoretical analysis, the dc/dc converter is a linear time-invariant (LTI) system. However, the dc/dc converter cannot maintain in an LTI system in actual operation, as the parameters of the critical components will degrade under different working conditions. In [3], the fragile components in power electronics converters include power device (MOSFET), capacitors, inductors, and resistors. Different types of components have different fault modes and failure mechanisms; the capacitance C tends to decrease and the Ron, RL, and ESR tend to increase with the increasing operation time in the dc/dc converter.

For the dc/dc converter, anomaly usually comes from two sources. One is the parameter degradation of the components in dc/dc converters, and the other one is the abnormal operation conditions, such as changing loads or the operation temperature. Based on the above analysis, there are three types of the states to be injected. The first type is the normal states, denoted as N1–N4, in which the parameter deviation of all components is less than the tolerance 5%. The second type is the anomalous states, in which the parameter deviation of all components is more than the tolerance 5%, denoted as AN1–AN6, AN7, and AN8 are the open and short faults. The third type of state is the anomalous states, denoted as AN9–AN10, caused by the load changes. The normal set and anomaly set are listed in Table IV.

To enhance the difference between the normal state and anomalous state, seven statistical features are used as the detection indexes. The extreme values of seven features based on the estimated output range are quickly calculated by a GA, which will increase the modeling time and the calculation consumption. The extreme values are listed in Table V.

The extreme values in Table V are the key criteria for detecting an anomaly in a dc/dc converter based on the proposed method. Seven features of each state are listed in Table VI.

In Table VI, all features of the normal states N1–N4 are in the normal output range. For the anomalous states, these cells with the bold fronts and green shadows indicate that the corresponding statistical features exceed the extreme values. Therefore, AN1–AN10 are distinguished as anomaly states because there is at least one feature deviating from the extreme values.

Table VII lists the comparison results among the proposed method, the original comparison mentioned in Section II, the estimation method mentioned in [7], and support vector data description (SVDD) method. SVDD is widely used as a fault classifier to detect anomalies and it adopts the same features as the proposed method. For the original comparison, the principle of the anomaly detection is that the output deviates from the normal threshold values, which are the output extreme values when all parameters of the components are in the tolerance 5%. For the estimation method in [7], it adopts the model to calculate the capacitance and ESR values. The anomalous states can be identified when the calculation values deviate from the tolerance range of these two parameters. The normal criterions of the proposed method and SVDD are acquired according to the established models.

The results state that the proposed method has the stronger identification ability of the normal and anomalous states than the other three methods. The limitations for three methods are as follows. At first, the outputs of the original comparison method do not be processed by the feature extraction. Therefore, this method can only identify the normal states and the anomalous states with the obvious difference from the normal state. It has a poor identification ability of the subtle anomalous states caused by the weak parameter degradation and the load changing. Then, the estimation method in [7] has two limitations, one is that

TABLE IV
NORMAL SET AND ANOMALY SET IN THE BUCK CONVERTER

	Number of degrading parameters	Parameters	Parameter deviation ratio
N1	1	Ron	-2%
N2	2	L	+2%
		RL	+3%
N3	2	C	-1%
		ESR	+4%
N4	3	Ron	+5%
		C	-5%
		ESR	+4%
AN1	1	Ron	+35%
AN2	2	L	+10%
		RL	+7%
AN3	3	C	-5%
		ESR	+6%
		Ron	+10%
AN4	4	C	-10%
		ESR	+7%
		L	+15%
		RL	+11%
AN5	4	C	-6%
		ESR	+12%
		L	+11%
		RL	+23%
AN6	5	C	-9%
		ESR	+13%
		L	+22%
		RL	+14%
		Ron	+11%
AN7	1	L	Open fault
AN8	1	C	Short fault
AN9	1	R (Load)	+10%
AN10	1	R (Load)	-8%

TABLE V
MAXIMUM AND MINIMUM VALUES OF SEVEN STATISTICAL FEATURES UNDER IDEAL CONDITION

	r	m	v	s	k	e	c
Max	0.181	2.605	0.055	0.446	1.268	22.55	17.92
Min	0.173	2.592	0.052	0.343	-1.483	22.53	-36.10

TABLE VI
SEVEN STATISTICAL FEATURES OF THE NORMAL AND ANOMALOUS SATES

	r	*m*	*v*	*s*	*k*	*e*	*c*
N1	0.175	2.601	0.052	0.423	1.215	22.53	11.56
N2	0.177	2.594	0.055	0.375	0.468	22.54	0.76
N3	0.180	2.592	0.054	0.437	0.591	22.55	12.04
N4	0.179	2.603	0.053	0.398	-1.160	22.53	-25.89
	r	*m*	*v*	*s*	*k*	*e*	*c*
AN1	**0.185**	**2.591**	0.052	0.412	-0.589	22.54	-11.05
AN2	**0.188**	2.599	0.053	0.368	**1.308**	22.55	-29.09
AN3	**0.190**	2.602	0.054	0.391	0.766	22.54	**19.23**
AN4	**0.215**	**2.583**	**0.051**	**0.475**	1.125	22.55	**28.12**
AN5	**0.231**	**2.675**	**0.045**	**0.513**	0.909	22.53	**32.95**
AN6	**0.272**	**2.713**	**0.059**	**0.575**	**3.013**	**22.72**	**28.12**
AN7	**0.011**	**0.478**	**0.159**	**0.675**	**7.495**	**32.25**	**58.15**
AN8	**0.024**	**0.036**	**0.018**	**0.276**	**-5.378**	**10.89**	**-45.18**
AN9	0.173	**2.493**	0.054	0.392	0.729	22.54	**-37.23**
AN10	0.179	**2.671**	0.052	0.432	0.816	22.53	**27.05**

TABLE VII
DETECTION RESULTS FOR SINGLE OUTPUT USING DIFFERENT METHODS UNDER THE IDEAL CONDITION

	The proposed method	Original signal comparison	Estimation methods Reference [7]	SVDD
N1	√	√	√	√
N2	√	√	×	√
N3	√	√	√	√
N4	√	√	×	√
AN1	√	×	√	×
AN2	√	×	√	×
AN3	√	×	×	×
AN4	√	×	√	√
AN5	√	√	√	√
AN6	√	√	√	√
AN7	√	√	√	√
AN8	√	√	√	√
AN9	√	×	×	×
AN10	√	×	×	×

"√" means that this state can be detected.
"×" means that this state cannot be detected.

the parameters of the other components except for the electric capacitor should be the nominal values when obtaining the accurate calculation values. The normal states N2 and N4 are improperly determined as the anomalous states. The other is that the accuracy of calculation values is strongly determined by the accuracy of the output. For the anomalous states AN3, AN9, and AN10, they are improperly determined as the normal states because the anomalous outputs deviate weakly from the normal output. Finally, the model established by SVDD has great identification ability of the normal state and the anomalous states caused by the large parameter degradation. The identification ability is not good for the anomalous sates caused by the weak parameter degradation.

To further compare the anomaly detection ability, Monte Carlo simulation is used here. The component tolerance is set to 5% and 200 simulation experiments are carried out. Table VIII lists the comparison results.

TABLE VIII
DETECTION RESULTS FOR MULTIPLE OUTPUTS USING DIFFERENT METHODS UNDER THE IDEAL CONDITION

	The proposed method	Original signal comparison	Estimation methods Reference [7]	SVDD
	Normal detection accuracy	Normal detection accuracy	Normal detection accuracy	Normal detection accuracy
N1	95.50%	95.50%	92.50%	98.50%
N2	95.00%	96.50%	51.50%	98.00%
N3	96.00%	97.00%	94.00%	97.50%
N4	94.50%	96.50%	44.50%	98.50%
	Anomaly detection accuracy	Anomaly detection accuracy	Anomaly detection accuracy	Anomaly detection accuracy
AN1	92.50%	64.00%	91.50%	55.00%
AN2	95.50%	59.50%	95.50%	57.50%
AN3	97.50%	69.50%	51.50%	75.00%
AN4	98.50%	76.50%	92.50%	89.50%
AN5	99.50%	90.50%	97.00%	95.00%
AN6	100.00%	98.00%	98.50%	100.00%
AN7	100.00%	100.00%	100.00%	100.00%
AN8	100.00%	100.00%	100.00%	100.00%
AN9	94.50%	69.50%	62.50%	71.50%
AN10	94.00%	56.50%	51.50%	67.50%

The results from Table VIII show that the proposed method can significantly increase the anomaly accuracy, especially for the anomaly states caused by the weak parameter degradation of the components.

2) Online Anomaly Detection Under Noise: The aforementioned normal outputs are obtained under ideal working conditions. In fact, noise and interference inevitably exist in the actual output of the dc/dc converter and derive from five types of sources: the low-frequency input ripple caused by the electrolytic capacitor, the high-frequency ripple caused by the high-frequency power switch circuit, common-mode ripple noise caused by the parasitic parameter, ultrahigh-frequency noise caused by the power component, and ripple noise caused by the closed-loop regulator [29]. The noise and interference may hinder the identification of the anomalous states. To simulate the actual outputs under different working conditions, this article adopts the normal outputs mixed with different amplitudes of the noise. There are four types of noise, whose amplitudes are ± 10, ± 25, ± 40, and ± 80 mV. These normal samples are used as training data to build the GPR model. The results are shown in Fig. 5.

In Fig. 5, different normal outputs can be included by the estimated normal output range. The GPR model can adjust the estimated range according to the actual output under different working conditions and decrease the effects of the noise and interference on the anomaly identification ability. Therefore, the GPR model is suitable for different working conditions, and the estimated normal output range is valid and effective.

To demonstrate the detection ability under the noise condition, the output with ± 40 mV noise is used as an example.

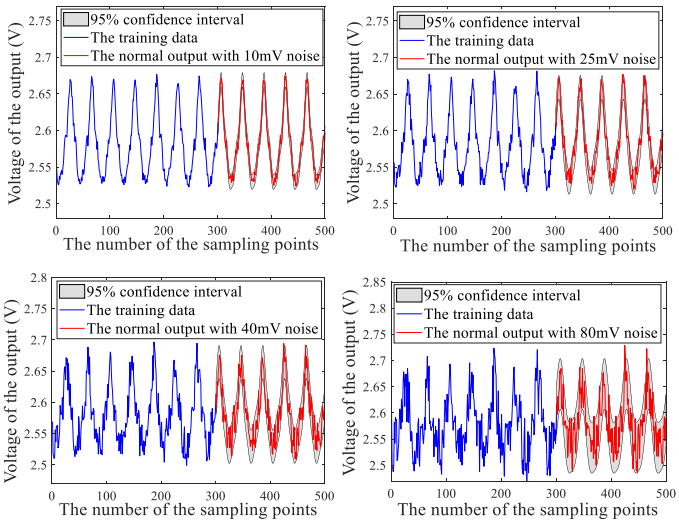

Fig. 5. Estimated normal output range based on the GPR model for normal output with various noise amplitudes.

TABLE IX
MAXIMUM AND MINIMUM VALUES OF SEVEN STATISTICAL FEATURES UNDER THE NOISE

	r	*m*	*v*	*s*	*k*	*e*	*c*
Max	0.176	2.589	0.059	0.686	0.781	22.55	19.08
Min	0.152	2.575	0.048	0.229	-1.948	22.51	-14.88

TABLE X
DETECTION RESULTS FOR SINGLE OUTPUT USING DIFFERENT METHODS UNDER NOISE

	The proposed method	Original signal comparison	Estimation methods Reference [7]	SVDD
N1	√	√	×	√
N2	√	√	×	√
N3	√	√	×	√
N4	√	√	×	√
AN1	√	×	×	×
AN2	√	×	×	×
AN3	√	×	×	×
AN4	√	×	√	×
AN5	√	×	√	×
AN6	√	√	√	√
AN7	√	√	√	√
AN8	√	√	√	√
AN9	√	×	×	×
AN10	√	×	×	×

"√" means that this state can be detected.
"×" means that this state cannot be detected.

The extreme values of the seven statistical features are listed in Table IX based on the proposed method.

The output for each state in Table IV is acquired under the noise condition. The comparison experiments are conducted and the detection results are shown in Table X.

Under the noise, the proposed method also has the stronger identification ability of the normal and anomalous states than the other three methods. Because of the noise in the output, some weak anomalous states may not be detected by the original comparison method and SVDD. For the estimation method, the noise existing in the output has the adverse effect on the accuracy of the output, so the detection results are worse than that under the ideal condition.

TABLE XI
DETECTION RESULTS FOR MULTIPLE OUTPUTS USING DIFFERENT METHODS UNDER NOISE

	The proposed method	Original signal comparison	Estimation methods Reference [7]	SVDD
	Normal detection accuracy	Normal detection accuracy	Normal detection accuracy	Normal detection accuracy
N1	93.50%	93.50%	83.50%	95.50%
N2	94.00%	94.50%	50.50%	95.00%
N3	94.00%	95.50%	85.00%	95.00%
N4	93.50%	94.00%	44.50%	95.50%
	Anomaly detection accuracy	Anomaly detection accuracy	Anomaly detection accuracy	Anomaly detection accuracy
AN1	91.00%	59.00%	85.50%	51.00%
AN2	95.50%	54.50%	89.00%	55.00%
AN3	95.00%	65.00%	51.50%	72.50%
AN4	96.00%	71.50%	89.50%	77.00%
AN5	95.50%	97.50%	95.00%	89.00%
AN6	97.00%	98.00%	94.50%	92.00%
AN7	100.00%	100.00%	100.00%	100.00%
AN8	100.00%	100.00%	100.00%	100.00%
AN9	92.50%	69.50%	60.50%	68.50%
AN10	92.00%	56.50%	49.50%	65.50%

In the simulation environment under the noise, the tolerance of the component has been set to 5%, 200 outputs are acquired by Monte Carlo simulation. The comparison results are shown in Table XI.

From Table XI, the proposed method can also obtain a high anomaly detection accuracy, especially for the anomaly states caused by the weak parameter degradation of the components. Compared with the results in the ideal simulation, the detection accuracy decreases because of the noise in the outputs.

3) Comparison of The Robustness: The article adopts statistical features to describe the output, which can enhance the difference between the normal and anomalous state. This is because the statistical feature expresses the entire changes of the output in the dc/dc converter rather than each local change of the outputs. The estimation effectiveness of statistical feature is unaffected by the local detail changes derived from accidental interference and noise. Therefore, this method can increase the anomaly detection ability and the robustness. An output with ±25 mV noise is used as an example, in Fig. 6, where the red line represents the output with the local interference, and the normal output range is obtained by GPR. A few output samples exceed the normal output range.

The comparison experiment is conducted to demonstrate the advantage of the statistical feature estimation. The comparison method is that the normal output with the local interference is directly compared with the normal output range point by point.

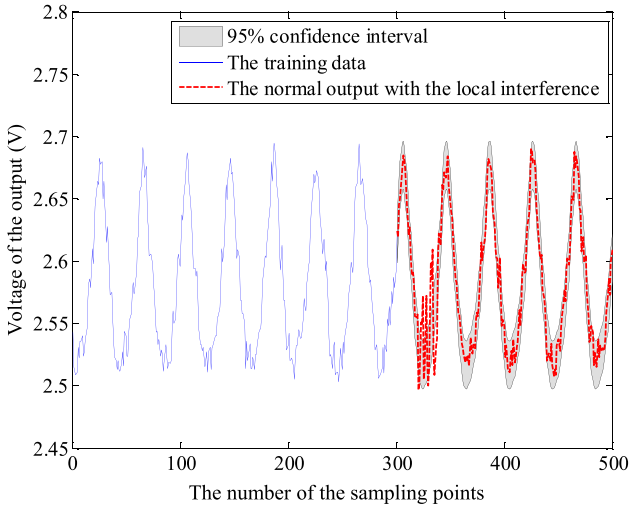

Fig. 6. Output with local interference.

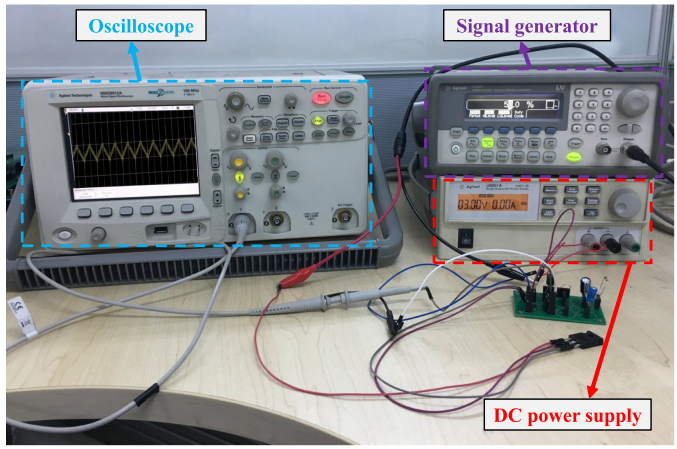

Fig. 7. Hardware experiment platform.

The principle of anomaly detection is that the output will be considered as an anomalous state once any one output sampling point exceeds the normal output range. The detection results are expressed as the number of actual output sampling points locating outside the estimated normal output range. For the actual output in Fig. 6, the result is 180/200, which means that there are 20 output sampling points exceeding the normal output range; then, this normal output with local interference is falsely identified as an anomalous state. The low normal identification ability leads to false alarms. When using statistical feature estimation, the number of statistical features exceeding the extreme values is used to express the anomaly detection results. The results are that none of the features exceeds the extreme values, which indicates that the output is the normal state. For the direct output comparison point by point, the reason of an incorrect detection result is that the direct output comparison shows local changes, the robustness to noise and interference is low. In fact, the parameter degradation of the component always has an effect on the entire changes of the output. The statistical feature estimation can express the trending changes of the output and can more clearly indicate the anomalous states than using a direct output comparison point by point. This demonstrates that statistical feature estimation has a high normal state identification ability and robustness to noise and interference.

4) Comparison of Operation Time: After sampling the outputs from the actual circuits, the process of anomaly detection is completed by MATLAB on a PC. The operation time includes the modeling time and detection time. Even though the modeling process consumes the most operation time, this process is only operated once before the detection process.

For the modeling time, two comparison experiments are conducted to validate the statement that the proposed method needs less modeling time. 1) For decreasing the modeling time, the proposed method uses the GA search to obtain the extreme values of seven features. A comparison experiment between the GA search and the related conference paper [28] is conducted. For example, the extreme statistical features in [28] are calculated by the randomly sampling 1000 output signals, the extreme values of each feature of these output signals are considered as the detection indexes to identify the anomalous state. The obtained extreme values are not accurate, and the calculation cost is high. In this article, the number of executions by a GA search is set to 200, because the extreme values maintain unchanged when 200 executions are performed. The large difference in the number of executions indicates that the GA search can significantly reduce the operation time, and the extreme values are more accurate than the conference paper [28]. 2) The second comparison experiment is conducted between SVDD and the proposed method. The operation time of the proposed method and SVDD are 11.657 and 14.265 s. The results show that the proposed method, compared with SVDD, can weakly reduce the modeling time.

For the detection time, only a simple comparison is implemented, so the detection time is short to microseconds. It will be very short for both SVDD and the proposed method. Therefore, the online anomalies can be quickly detected based on the established models.

B. Hardware Experiment

The experimental environment of the software is too ideal to simulate the real environment where a circuit operates. In addition, noise and interference inevitably exist in the actual output of the dc/dc converter. A hardware experiment platform is built to verify the effectiveness of the proposed method. The hardware experiment circuit involves a buck converter. Fig. 7 shows the hardware experiment platform.

The hardware experiment platform consists of three major instruments. The dc signal source is an Agilent U8001 A single output dc power supply that supplies +3 V power to the buck converter. The Agilent 33220-A signal generator generates the PWM signal that controls the MOSFET transistor IRF 150. The period of the PWM signal is set to 50 μs, and the duty cycle is set to 50%. The MOS6012 A oscilloscope is used to show the waveforms of the output and export the output data into the computer.

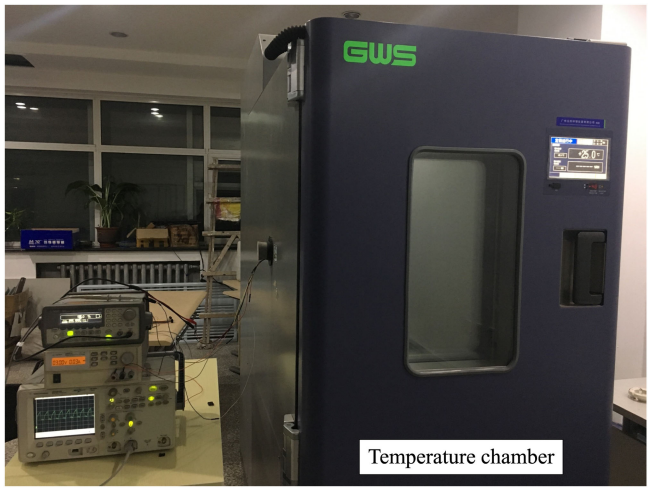

Fig. 8. Experiment platform in the temperature chamber.

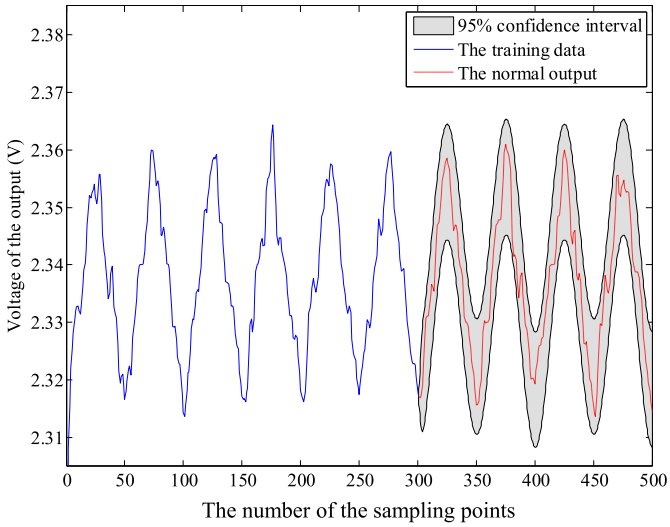

Fig. 9. Estimated normal output based on GPR model in the hardware experiment.

For the dc/dc converter, the anomalies are derived from the changing load conditions and the degrading parameters of the components. In this article, to validate the effectiveness and practicability of the proposed method, the hardware experiments are conducted in two types of operating conditions, including ambient temperature and different operating temperatures.

1) Online Anomaly Detection Under Ambient Temperature: In the hardware experiment, first, the hardware circuit is placed in a temperature chamber, the operating temperature is set as 25 °C to keep the circuit under ambient temperature. The hardware experiment platform in the temperature chamber is shown as Fig. 8. Then, the number of the normal sample points and the sampling period of the output signal are set to 500 and 1 μs, respectively. The initial 300 points are taken as the training data, and the normal output range is determined using GPR. Fig. 9 shows the normal output range. Finally, the extreme values of seven statistical features are quickly calculated from the normal output range by the GA. Seven features are listed in Table XII.

TABLE XII
MAXIMUM AND MINIMUM VALUES OF SEVEN STATISTICAL FEATURES IN HARDWARE EXPERIMENT

	r	m	v	s	k	e	c
Max	0.054	2.339	0.088	0.325	0.342	21.44	53.01
Min	0.049	2.335	0.064	0.116	-1.275	21.43	-46.00

TABLE XIII
ANOMALY SET IN THE HARDWARE EXPERIMENT

	Number of degrading parameters	Parameters	Values of the parameters
AN1	2	C	6.935 μF
		ESR	1.516 Ω
AN2	2	C	4.273 μF
		ESR	0.941 Ω
AN3	2	C	3.912 μF
		ESR	0.987 Ω
AN4	2	C	3.597 μF
		ESR	1.034 Ω
AN5	2	C	3.357 μF
		ESR	1.081 Ω
AN6	2	C	3.133 μF
		ESR	1.129 Ω
AN7	2	C	2.938 μF
		ESR	1.176 Ω
AN8	2	C	2.231 μF
		ESR	1.786 Ω
AN9	1	R (Load)	54 Ω
AN10	1	R (Load)	47 Ω
AN11	1	R (Load)	60 Ω
AN12	1	R (Load)	44 Ω

TABLE XIV
AVERAGE ANOMALY DETECTION ACCURACY WITH DIFFERENT DETECTION METHODS IN HARDWARE EXPERIMENT

	The proposed method	Original signal comparison	Estimation methods Reference [7]	SVDD
Average anomaly detection accuracy	91.00%	59.00%	85.50%	51.00%

When the dc/dc converter operates under ambient temperature, the anomalous states derive from the degrading parameters of the components and the changing load. Hence, in this article, the anomalies are caused by the changing parameters of the electrolytic capacitor and the different load conditions. The normal capacitance and ESR values used in this article are 4.7 μF and 0.893 Ω, which, combined with 47 μF, are used to construct the anomalous states. The values of the capacitance and ESR are measured by the *LCR* measurement instrument MT 4080 A. The anomalous set is shown in Table XIII.

For the hardware experiments, the fault or anomalous samples are insufficient, the result is defined as the average detection accuracy of all the anomalous states. The average anomalous detection accuracy is shown in Table XIV.

TABLE XV
ANOMALY DETECTION ACCURACY BY USING DIFFERENT METHODS IN HARDWARE EXPERIMENT

	The proposed method	Original signal comparison	Estimation methods Reference [7]	SVDD
Temperature stress	Anomaly detection accuracy	Anomaly detection accuracy	Anomaly detection accuracy	Anomaly detection accuracy
35°C	88.50%	42.50%	52.50%	57.50%
45°C	90.00%	53.00%	56.50%	63.50%
50°C	91.50%	55.50%	59.00%	70.00%
55°C	92.00%	60.50%	61.50%	74.00%
60°C	94.00%	73.00%	65.50%	77.50%
65°C	95.50%	78.50%	75.00%	85.50%
70°C	96.50%	85.50%	85.50%	93.00%
75°C	100.00%	90.50%	93.50%	98.50%
80°C	100.00%	98.50%	98.00%	100.00%

The results in Table XIV demonstrate that the proposed method, compared with the other three methods, can increase the anomaly detection accuracy and has higher anomaly identification ability in actual operation.

For the results in Table XIV, the modeling time of the proposed method and SVDD mainly consumes in the operation process, the modeling process is the same as the simulation experiment, so the modeling time is still 11.657 and 14.265 s. For the detection time, it will be very short for both SVDD and the proposed method. Because only a simple comparison is implemented, it may be short to microseconds.

2) Online Anomaly Detection Under Abnormal Operating Temperatures: In actual operation, the environmental stresses of the dc/dc converter may not keep stable. In this article, the abnormal temperature is chosen as the abnormal environment stress. When the converter operates in the abnormal temperature for some time, the abnormal environment stress may accelerate the parameter degradation of the components in the dc/dc converter and the load changing. The causes of anomalous states are unclear and complex. The abnormal stresses include 35, 45, 50, 55, 60, 65, 70, 75, and 80 °C. The output of dc/dc converter is considered as the normal state at the 25 °C operation temperature. First, nine hardware circuits of the buck converter are prepared to operate under nine temperature stresses. Then, for each circuit, the normal output range is estimated by GPR using the normal output at a 25 °C operation temperature. Finally, nine circuits are placed into the temperature chamber to operate under nine temperature stresses. The duration time of the temperature experiment is 72 h, and 200 outputs of each circuit are obtained. The anomaly detection accuracy based on the proposed method and three comparison methods are shown in Table XV.

From Table XV, the anomaly detection accuracy of the proposed method is higher than that of the other three methods, which demonstrates that the proposed method can significantly increase the anomaly detection accuracy and has high anomaly identification ability.

In summary, the results of the above hardware experiments show that the proposed method can detect not only the anomalous states caused by the original defects of the components and changing operation conditions, but also the occasional anomaly derived from abnormal load conditions. These results demonstrate the effectiveness and practicability of the proposed method.

IV. CONCLUSION

This article presents a method of online anomaly detection by statistical feature estimation using GPR and a GA for a dc/dc converter with a known or unknown circuit structure. The normal output range is estimated based on GPR. The extreme values of seven statistical features are calculated by a GA using the normal output range. In the simulation experiments, the method is applied to a buck converter under ideal and noisy conditions. All normal states and anomalous states can be effectively identified using the seven statistical features estimation. It is demonstrated that the normal output range based on GPR is suitable for application in various working conditions. Compared with original comparison method, estimation method, and SVDD, the proposed method has higher anomaly detection ability. Then, relative to the direct output comparison point by point, statistical feature estimation can enhance the detection ability of the anomalous states and the robustness. The use of a GA optimum search algorithm not only can decrease the modeling time and the calculation consumption, but also can obtain relatively accurate extreme values. Finally, when the anomaly detection method is used on a hardware circuit, the anomalous states caused by the parameter degradation of the components and changing operating conditions can be effectively and accurately identified. The simulation and hardware results demonstrate that the proposed method can quickly and effectively detect online anomalies in a dc/dc converter regardless of whether the circuit structure is known. This novel method is appropriate for applications that require fast online anomaly detection and has considerable practical value. At present, the proposed method only can realize the anomaly detection of dc/dc converter, and it cannot identify the degradation parameters and determine the fault location. These relative research works are the main work in the future.

REFERENCES

[1] B. Mohandes, M. S. E. Moursi, N. Hatziargyriou, and S. E. Khatib, "A review of power system flexibility with high penetration of renewables," *IEEE Trans. Power Syst.*, vol. 34, no. 4, pp. 3140–3155, Jul. 2019.
[2] J. Falck, C. Felgemacher, A. Rojko, M. Liserre, and P. Zacharias, "Reliability of power electronic systems: An industry perspective," *IEEE Ind. Electron. Mag.*, vol. 12, no. 2, pp. 24–35, Jun. 2018.
[3] S. Yang, A. Bryant, P. Mawby, D. Xiang, L. Ran, and P. Tavner, "An industry-based survey of reliability in power electronic converters," in *Proc. IEEE Energy Convers. Congr. Expo.*, Sep. 2009, pp. 3151–3157.
[4] M. K. Alam and F. H. Khan, "Reliability analysis and performance degradation of a boost converter," *IEEE Trans. Ind. Appl.*, vol. 50, no. 6, pp. 3986–3994, Nov. 2014.
[5] A. Shrivastava, M. H. Azarian, C. Morillo, B. Sood, and M. Pecht, "Detection and reliability risks of counterfeit electrolytic capacitors," *IEEE Trans. Rel.*, vol. 63, no. 2, pp. 468–479, Jun. 2014.
[6] K. Yao *et al.*, "A noninvasive online monitoring method of output capacitor's C and ESR for DCM flyback converter," *IEEE Trans. Power Electron.*, vol. 34, no. 6, pp. 5748–5763, Jun. 2019.
[7] K. Yao, W. Tang, W. Hu, and J. Lyu, "A current-sensorless online ESR and C identification method for output capacitor of buck converter," *IEEE Trans. Power Electron.*, vol. 30, no. 12, pp. 6993–7005, Dec. 2015.

[8] K. Yao, W. Tang, X. Bi, and J. Lyu, "An online monitoring scheme of dc-link capacitor's ESR and C for a boost PFC converter," *IEEE Trans. Power Electron.*, vol. 31, no. 8, pp. 5944–5951, Aug. 2016.
[9] M. W. Ahmad, N. Agarwal, and S. Anand, "Online monitoring technique for aluminum electrolytic capacitor in solar PV-based DC system," *IEEE Trans. Ind. Electron.*, vol. 63, no. 11, pp. 7059–7066, Nov. 2016.
[10] M. W. Ahmad, N. Agarwal, P. N. Kumar, and S. Anand, "Low-frequency impedance monitoring and corresponding failure criteria for aluminum electrolytic capacitors," *IEEE Trans. Ind. Electron.*, vol. 64, no. 7, pp. 5657–5666, Jul. 2017.
[11] J. Hannonen, J. Honkanen, J. Strom, T. Karkkainen, S. Raisanen, and P. Silventoinen, "Capacitor aging detection in a dc–dc converter output stage," *IEEE Trans. Ind. Appl.*, vol. 52, no. 4, pp. 3224–3233, Jul. 2016.
[12] H. Nakao, Y. Yonezawa, T. Sugawara, Y. Nakashima, and F. Kurokawa, "Online evaluation method of electrolytic capacitor degradation for digitally controlled SMPS failure prediction," *IEEE Trans. Power Electron.*, vol. 33, no. 3, pp. 2552–2558, Mar. 2018.
[13] A. M. R. Amaral and A. J. M. Cardoso, "On-line fault detection of aluminium electrolytic capacitors, in step-down dc-dc converters, using input current and output voltage ripple," *IET Power Electron.*, vol. 5, no. 3, pp. 315–322, Mar. 2012.
[14] M. Shahbazi, E. Jamshidpour, P. Poure, S. Saadate, and M. R. Zolghadri, "Open- and short-circuit switch fault diagnosis for nonisolated dc–dc converters using field programmable gate array," *IEEE Trans. Ind. Electron.*, vol. 60, no. 9, pp. 4136–4146, Sep. 2013.
[15] X. Pu, T. H. Nguyen, D. Lee, K. Lee, and J. Kim, "Fault diagnosis of dc-link capacitors in three-phase ac/dc PWM converters by online estimation of equivalent series resistance," *IEEE Trans. Ind. Electron.*, vol. 60, no. 9, pp. 4118–4127, Sep. 2013.
[16] T. H. Nguyen and D. Lee, "Deterioration monitoring of dc-link capacitors in ac machine drives by current injection," *IEEE Trans. Power Electron.*, vol. 30, no. 3, pp. 1126–1130, Mar. 2015.
[17] S. Mohagheghi, R. G. Harley, T. G. Habetler, and D. Divan, "Condition monitoring of power electronic circuits using artificial neural networks," *IEEE Trans. Power Electron.*, vol. 24, no. 10, pp. 2363–2367, Oct. 2009.
[18] H. A. H. Soliman, H. Wang, B. S. A. Gadalla, and F. Blaabjerg, "Artificial neural network algorithm for condition monitoring of dc-link capacitors based on capacitance estimation," *Renewable Energy Sustain. Develop.*, vol. 1, no. 2, pp. 294–299, 2015.
[19] A. G. Abo-Khalil and D. Lee, "DC-link capacitance estimation in ac/dc/ac PWM converters using voltage injection," *IEEE Trans. Ind. Appl.*, vol. 44, no. 5, pp. 1631–1637, Sep. 2008.
[20] K. Laadjal, M. Sahraoui, A. J. M. Cardoso, and A. M. R. Amaral, "Online estimation of aluminum electrolytic-capacitor parameters using a modified prony's method," *IEEE Trans. Ind. Appl.*, vol. 54, no. 5, pp. 4764–4774, Sep./Oct. 2018.
[21] E. Farjah, H. Givi, and T. Ghanbari, "Application of an efficient Rogowski coil sensor for switch fault diagnosis and capacitor ESR monitoring in nonisolated single-switch dc–dc converters," *IEEE Trans. Power Electron.*, vol. 32, no. 2, pp. 1442–1456, Feb. 2017.
[22] A. M. Airabella, G. G. Oggier, L. E. Piris-Botalla, C. A. Falco, and G. O. Garcła, "Semi-conductors faults analysis in dual active bridge dc/dc converter," *IET Power Electron.*, vol. 9, no. 6, pp. 1103–1110, 2016.
[23] S. Nie, X. Pei, Y. Chen, and Y. Kang, "Fault diagnosis of PWM dc–dc converters based on magnetic component voltages equation," *IEEE Trans. Power Electron.*, vol. 29, no. 9, pp. 4978–4988, Sep. 2014.
[24] C. K. Williams and C. E. Rasmussen, "Gaussian processes for regression," in *Proc. Adv. Neural Inf. Process. Syst.*, 1996, pp. 514–520.
[25] L. Yuan, Y. He, J. Huang, and Y. Sun, "A new neural-network-based fault diagnosis approach for analog circuits by using kurtosis and entropy as a preprocessor," *IEEE Trans. Instrum. Meas.*, vol. 59, no. 3, pp. 586–595, Mar. 2010.
[26] C. Gao, J.-Y. Huang, Y. Sun, and S.-l. Diao, "Particle swarm optimization based RVM classifier for non-linear circuit fault diagnosis," *J. Central South Univ.*, vol. 19, no. 2, pp. 459–464, 2012.
[27] L. Bing, W. Xian, L. Min, and H. Wang, "Improved diagnostics for the incipient faults in analog circuits using LSSVM based on PSO algorithm with mahalanobis distance," *Neurocomputing*, vol. 133, no. 10, pp. 237–248, 2014.
[28] Y. Jiang, Y. Yu, and X. Peng, "Online anomaly detection in switching-mode power module using statistical property features comparison and gaussian process regression," in *Proc. Int. Conf. Sens., Diagnostics, Prognostics, Control*, Aug. 2018, pp. 320–327.
[29] M. Tehranipoor and K. M. Butler, "Power supply noise: A survey on effects and research," *IEEE Des. Test Comput.*, vol. 27, no. 2, pp. 51–67, Mar. 2010.

Yueming Jiang was born in Harbin, China, in 1989. She received the B.S. and M.S. degrees in measuring & control technology and instrumentation from the Harbin University of Science and Technology, Harbin, China, in 2011 and 2014, respectively. She is currently working toward the Ph.D. degree with the School of Electronics and Information Engineering, Harbin Institute of Technology, Harbin, China.

Her research interests include the detection and diagnosis of incipient fault in analog circuit, feature selection of analog fault, and component degradation modeling.

Yang Yu (Senior Member, IEEE) received the B.S., M.S. and Ph.D. degrees from the Department of Test and Control Engineering, Harbin Institute of Technology (HIT), Harbin, China, in 2002, 2004, and 2008, respectively.

From 2015 to 2016, she was a Visiting Scholar with Duke University, Durham, NC, USA. She is currently an Associate Professor with the Department of Automatic Test and Control, School of Electronics and Information Engineering, HIT. She holds 21 granted China patents and has authored over 30 publications in major journals and conference proceedings on electronic test technology. Her current research interests include automatic testing, test technology for 3D ICs, and diagnostic and prognostics for electronic systems.

Xiyuan Peng received the Ph.D. degree in instrumentation science and technology from the Harbin Institute of Technology (HIT), Harbin, China, in 1992.

He is currently a Full Professor with Department of Test and Control Engineering, School of Electronics and Information Engineering, HIT. His current research interests include automatic test technologies, advanced diagnostics, and prognostics.